

# Electron- or Hole-Transporting Nature Selected by Side-Chain-Directed $\pi$ -Stacking Geometry: Liquid Crystalline Fused Metalloporphyrin Dimers

Tsuneaki Sakurai,<sup>†</sup> Kentaro Tashiro,<sup>‡</sup> Yoshihito Honsho,<sup>§</sup> Akinori Saeki,<sup>§</sup> Shu Seki,<sup>§</sup> Atsuhiko Osuka,<sup>||</sup> Atsuya Muranaka,<sup>#</sup> Masanobu Uchiyama,<sup>#,⊥</sup> Jungeun Kim,<sup>∇</sup> Sunyeo Ha,<sup>⊗</sup> Kenichi Kato,<sup>||</sup> Masaki Takata,<sup>∇,⊗,¶</sup> and Takuzo Aida<sup>\*†</sup>

<sup>†</sup>School of Engineering, The University of Tokyo, 7-3-1 Hongo, Bunkyo-ku, Tokyo 113-8656, Japan

<sup>‡</sup>National Institute for Materials Science, 1-1 Namiki, Tsukuba, Ibaraki 305-0044, Japan

<sup>§</sup>Graduate School of Engineering, Osaka University, 2-1 Yamadaoka, Suita, Osaka 565-0871, Japan

<sup>||</sup>Graduate School of Science, Kyoto University, Sakyo-ku, Kyoto 606-8502, Japan

<sup>#</sup>Institute of Physical and Chemical Research, RIKEN, 2-1 Hirosawa, Wako-shi, Saitama 351-0198, Japan

<sup>⊥</sup>Graduate School of Pharmaceutical Sciences, The University of Tokyo, 7-3-1 Hongo, Bunkyo-ku, Tokyo 113-0033, Japan

<sup>∇</sup>Japan Synchrotron Radiation Research Institute (JASRI), 1-1-1 Kouto, Sayo-cho, Sayo-gun, Hyogo 679-5198, Japan

<sup>⊗</sup>Graduate School of Frontier Sciences, The University of Tokyo, 5-1-5, Kashiwanoha, Kashiwa, Chiba 277-8561, Japan

<sup>¶</sup>RIKEN SPring-8 Center, 1-1-1 Kouto, Sayo-cho, Sayo-gun, Hyogo 679-5148, Japan

**S** Supporting Information

**ABSTRACT:** Novel liquid crystalline (LC) semiconductors were prepared from the copper complex of a fused porphyrin dimer as the electroactive core by attaching to its periphery dodecyl and semifluoroalkyl side chains site-specifically ( $P\equiv P_{\text{hetero}}$ ) and semifluoroalkyl side chains alone ( $P\equiv P_{\text{homo}}$ ). The former and latter formed rectangular columnar and orthorhombic LC mesophases, respectively, where the stacking geometries of the  $\pi$ -conjugated core are quite different from one another. Although the  $\pi$ -electronic properties of the core units in  $P\equiv P_{\text{hetero}}$  and  $P\equiv P_{\text{homo}}$  in solution are substantially identical to one another, transient photocurrent profiles of their LC states under time-of-flight conditions clearly showed that  $P\equiv P_{\text{hetero}}$  behaves as an n-type semiconductor, whereas  $P\equiv P_{\text{homo}}$ , in contrast, behaves as a p-type semiconductor.

In general, whether organic semiconductors transport electrons or holes has been considered to be determined mostly by the intrinsic redox properties of their constituent electroactive molecules.<sup>1</sup> Therefore, diversification of the range of n- and p-type organic semiconductors totally relies on the development of new  $\pi$ -conjugated structural motifs.<sup>2</sup> Toward this general understanding, we report here that, by tailoring assembly-directing side chains, both n- and p-type liquid crystalline (LC) semiconductors can be obtained from a single  $\pi$ -conjugated motif.

The electroactive core unit employed in the present work is the Cu complex of a triply fused porphyrin dimer adopting a characteristic oblong disk shape (Figure 1). Triply fused metalloporphyrin oligomers are interesting  $\pi$ -conjugated motifs, particularly for photovoltaic applications, because of their extraordinary high absorptivities toward sunlight, covering from ultraviolet up to near-infrared wavelength regions.<sup>3</sup> In 2008, we reported the

first LC version of this family, which carries dodecyl side chains on one Cu porphyrin unit and triethylene glycol (TEG) side chains on the other.<sup>4</sup> This particular heterotropic design was essential for the liquid crystal formation, since a prototype of this compound carrying only dodecyl side chains did not form a LC assembly but rather an amorphous solid. Although most porphyrin-based materials have been reported to show a hole-transporting property,<sup>5</sup> the above LC material, in contrast, behaved as an n-type semiconductor.<sup>4</sup> In the present work, this unexpected observation prompted us to investigate if the electron-transporting nature of this material is intrinsic to the core unit of the LC molecule or its particular peripheral design. In order to address this issue, we newly synthesized heterotropically fused  $P\equiv P_{\text{hetero}}$  along with homotropic  $P\equiv P_{\text{homo}}$  (Figure 1) by using semifluoroalkyl side chains instead of the TEG chains,<sup>6</sup> since fluorinated hydrocarbons are immiscible, just like TEG, with hydrocarbons and also have a very strong self-assembling nature.<sup>7</sup> Fortunately, both compounds formed a LC mesophase with a  $\pi$ -stacked columnar structure. However, to our surprise, their preferences for carrier species were totally opposite to one another.

Differential scanning calorimetry (DSC; Figure S4) of  $P\equiv P_{\text{hetero}}$ , on its second heating, displayed a LC mesophase ranging from  $-26$  to  $163$  °C (Figure 1). This LC temperature range is much wider than that of its TEG version ( $-17$  to  $99$  °C) previously reported.<sup>4</sup> Likewise,  $P\equiv P_{\text{homo}}$  formed a LC mesophase in a temperature range from  $-32$  to  $199$  °C (Figures 1 and S4). Polarized optical microscopy (POM) of both  $P\equiv P_{\text{hetero}}$  (Figure 2a) and  $P\equiv P_{\text{homo}}$  (Figure 2b) showed a clear dendritic texture typical of columnar LCs. In X-ray diffraction (XRD) analysis upon synchrotron radiation,  $P\equiv P_{\text{hetero}}$  at  $30$  °C displayed an

Received: February 10, 2011

Published: April 08, 2011

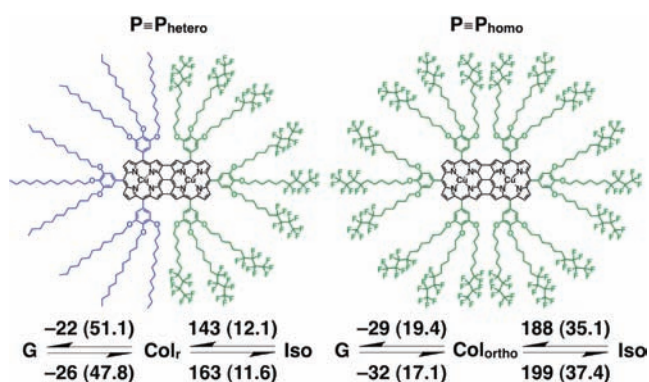


**Figure 1.** Molecular structures and phase transition temperatures ( $^{\circ}\text{C}$ ) of copper complexes of fused porphyrin dimers  $\text{P}\equiv\text{P}_{\text{hetero}}$  and  $\text{P}\equiv\text{P}_{\text{homo}}$ . Transition enthalpies ( $\text{kJ mol}^{-1}$ ) are given in parentheses.

intense diffraction peak at  $2\theta = 1.05^{\circ}$  ( $d = 59.1 \text{ \AA}$ ) along with several minor peaks in a wider-angle region (Figure 2c and Table S1). As in the case of the heterotropic TEG version,<sup>4</sup> these diffractions were successfully indexed to a 2D rectangular lattice with a symmetry group of  $p2mg$ ,<sup>8</sup> where lattice parameters  $a$  and  $b$  were 59.1 and 32.5  $\text{\AA}$ , respectively (Figure S3). In sharp contrast,  $\text{P}\equiv\text{P}_{\text{homo}}$  carrying semifluoroalkyl side chains alone at  $170^{\circ}\text{C}$  showed a crystal-like diffraction pattern (Figure 2d and Table S1), which was indexed to a 3D orthorhombic lattice<sup>9</sup> with lattice parameters  $a$ ,  $b$ , and  $c$  of 70.9, 28.4, and 20.1  $\text{\AA}$ , respectively. Due to their LC characters, both  $\text{P}\equiv\text{P}_{\text{hetero}}$  and  $\text{P}\equiv\text{P}_{\text{homo}}$  in their mesophases are shearable.<sup>9b</sup>

By means of variable-temperature absorption spectroscopy in the film state, we found that the  $\pi$ -stacking geometries of the fused Cu porphyrin core in these LC mesophases are different from each other. Porphyrin derivatives are known to change their absorption spectral profiles upon  $\pi$ -stacking.<sup>10</sup> An isotropic melt of  $\text{P}\equiv\text{P}_{\text{hetero}}$  at  $150^{\circ}\text{C}$  showed two characteristic Soret absorption bands at 407 and 561 nm (Figure 2e, red).<sup>3</sup> When the hot melt of  $\text{P}\equiv\text{P}_{\text{hetero}}$  was cooled to allow the isotropic-to-LC phase transition, a color change from dark purple to reddish brown resulted. Accordingly, the longer-wavelength Soret band, on stepwise cooling from 150 to  $125^{\circ}\text{C}$ , showed a 10-nm blue shift hypochromically. This spectral change took place abruptly around the phase transition temperature (Figure 2e). All these features are analogous to those observed for the TEG version of  $\text{P}\equiv\text{P}_{\text{hetero}}$ .<sup>4</sup> Although the absorption spectral profile of an isotropic melt of  $\text{P}\equiv\text{P}_{\text{homo}}$  at  $205^{\circ}\text{C}$  (Figure 2f, red), displaying two Soret bands at 407 and 564 nm, was just like that of  $\text{P}\equiv\text{P}_{\text{hetero}}$  (*vide ante*), the spectra of these compounds in the LC state were quite different from one another. When  $\text{P}\equiv\text{P}_{\text{homo}}$  was cooled to  $185^{\circ}\text{C}$  to allow the isotropic-to-LC phase transition, its Soret bands both became less intense (Figure 2f). Furthermore, in sharp contrast with the case of  $\text{P}\equiv\text{P}_{\text{hetero}}$ , the longer-wavelength Soret band exhibited an 8-nm red shift, with a new shoulder around 660 nm. Hence, it is clear that the  $\pi$ -stacking geometry of  $\text{P}\equiv\text{P}_{\text{homo}}$  in the LC state differs from that of  $\text{P}\equiv\text{P}_{\text{hetero}}$ .

$\pi$ -Conjugated molecules usually stack with an offset geometry in order to minimize repulsion of  $\pi$ -clouds.<sup>11</sup> Considering the heterotropic and homotropic substitution patterns of these LC molecules, along with reported examples with monomeric porphyrins,<sup>12</sup> we suggest columnar structures (a) and (b) in Figure 3 for  $\text{P}\equiv\text{P}_{\text{hetero}}$  and  $\text{P}\equiv\text{P}_{\text{homo}}$  in the LC state, respectively, where

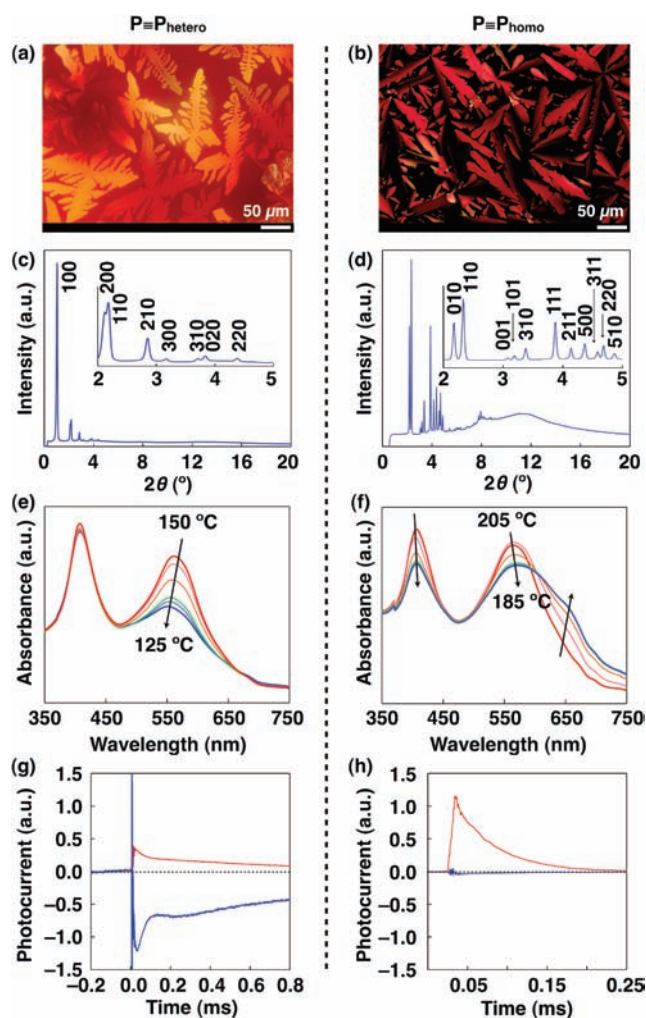


**Figure 2.** Characterization and properties of  $\text{P}\equiv\text{P}_{\text{hetero}}$  and  $\text{P}\equiv\text{P}_{\text{homo}}$  in their liquid crystalline (LC) mesophases. Polarized optical micrographs of (a)  $\text{P}\equiv\text{P}_{\text{hetero}}$  at  $150^{\circ}\text{C}$  and (b)  $\text{P}\equiv\text{P}_{\text{homo}}$  at  $185^{\circ}\text{C}$ . X-ray diffraction patterns of (c)  $\text{P}\equiv\text{P}_{\text{hetero}}$  at  $30^{\circ}\text{C}$  and (d)  $\text{P}\equiv\text{P}_{\text{homo}}$  at  $170^{\circ}\text{C}$ . The wavelength of incident X-ray was 1.08  $\text{\AA}$ . Changes in absorption spectra of (e)  $\text{P}\equiv\text{P}_{\text{hetero}}$  on cooling from  $150$  to  $125^{\circ}\text{C}$  and (f)  $\text{P}\equiv\text{P}_{\text{homo}}$  on cooling from  $205$  to  $185^{\circ}\text{C}$ . Typical transient photocurrent profiles at  $25^{\circ}\text{C}$  of (g)  $\text{P}\equiv\text{P}_{\text{hetero}}$  (sample thickness,  $3.3 \mu\text{m}$ ; electric field,  $0.94 \times 10^4 \text{ V cm}^{-1}$ ) and (h)  $\text{P}\equiv\text{P}_{\text{homo}}$  (sample thickness,  $19 \mu\text{m}$ ; electric field,  $6.0 \times 10^4 \text{ V cm}^{-1}$ ) for electron (blue) and hole (red).

column (a) is formed by offset stacking of the  $\pi$ -conjugated core with a “slipped geometry”, while column (b) is formed by offset stacking of the  $\pi$ -conjugated core with a “twisted geometry”. As discussed already for the TEG version of  $\text{P}\equiv\text{P}_{\text{hetero}}$ ,<sup>4</sup> which forms a rectangular columnar mesophase just as  $\text{P}\equiv\text{P}_{\text{hetero}}$ , column (a) seems to be the only possible structure that can cope with both stacking of the  $\pi$ -conjugated core and segregation of its two incompatible side chains. On the other hand, the twisted geometry in column (b) is a likely candidate for homotropically substituted  $\text{P}\equiv\text{P}_{\text{homo}}$ , since it allows for the formation of a continuous array of the highly self-associating semifluoroalkyl side chains around the column. In contrast, this geometry is unlikely for  $\text{P}\equiv\text{P}_{\text{hetero}}$ , because segregation of the two incompatible side chains is not allowed. Based on spectral simulation,<sup>6</sup> a dimer model for column (a) with a slipped geometry suggests

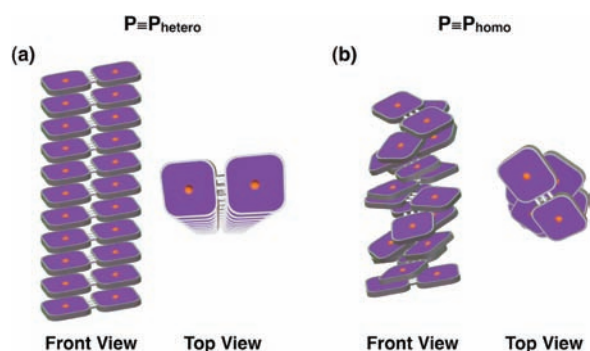


**Figure 3.** Schematic illustrations of the columnar structures ( $\pi$ -stacked core parts) proposed for the (a) rectangular and (b) orthorhombic columnar LC mesophases of  $P\equiv P_{\text{hetero}}$  and  $P\equiv P_{\text{homo}}$ , respectively. Judging from the XRD patterns (Figure 2c,d), the LC columns of  $P\equiv P_{\text{homo}}$  and  $P\equiv P_{\text{hetero}}$  are likely disordered along the columnar axis.

a blue shift of the Soret band, as observed for assembled  $P\equiv P_{\text{hetero}}$ , when the translational operation is made along the shorter axes of the  $\pi$ -conjugated units (Figure S5). If this operation is made along the longer axes, a blue shift can be expected only when the displacement is marginal (Figure S6). On the other hand, a  $\pi$ -stacked dimer model for column (b) with a twisted geometry suggests a spectral red shift, as observed for assembled  $P\equiv P_{\text{homo}}$ , when the dihedral angle lies in a range of 60–90° (Figure S7).<sup>4</sup>

We measured photocurrent profiles of  $P\equiv P_{\text{hetero}}$  and  $P\equiv P_{\text{homo}}$  in their LC states (25 °C) using a time-of-flight (TOF) technique. As shown in Figure 2g (blue),  $P\equiv P_{\text{hetero}}$  displayed an explicit n-type semiconducting character, where the electron mobility under an applied electric field of  $0.94 \times 10^4 \text{ V cm}^{-1}$  was evaluated as  $1.3 \times 10^{-3} \text{ cm}^2 \text{ V}^{-1} \text{ s}^{-1}$  (Figure S8).<sup>6</sup> Although the TOF profile also showed a small p-type signature, the photocurrent was too small to evaluate.<sup>13</sup> To our surprise,  $P\equiv P_{\text{homo}}$ , in sharp contrast with  $P\equiv P_{\text{hetero}}$ , behaved as a p-type semiconductor. In the TOF profile of  $P\equiv P_{\text{homo}}$  in its LC mesophase, a photocurrent appeared only when the applied electrical bias was positive (Figure 2h, red). In accordance with this observation, transient absorption spectroscopy (TAS)<sup>14</sup> of  $P\equiv P_{\text{homo}}$  (Figure S12) showed an absorption band around 690 nm, which can be assigned to radical cation species  $P\equiv P_{\text{homo}}^{\bullet+}$  by reference to the differential spectral profile between chemically generated  $P\equiv P_{\text{homo}}^{\bullet+}$  and neutral  $P\equiv P_{\text{homo}}$  (Figure S12).<sup>6</sup> The hole mobility, observed at an electric field strength of  $6.0 \times 10^4 \text{ V cm}^{-1}$  in the TOF experiment, was evaluated as  $4.3 \times 10^{-3} \text{ cm}^2 \text{ V}^{-1} \text{ s}^{-1}$  (Figure S8).<sup>6</sup> From these observations, whether the fused Cu porphyrin dimer core transports electron or hole in the LC state appears to be determined by its side chains.

In a good solvent such as  $\text{CH}_2\text{Cl}_2/\text{C}_6\text{H}_5\text{CF}_3$  (2/1 v/v), the absorption spectral profile (Figure S13) and differential pulse voltammogram (Figure S14) of  $P\equiv P_{\text{hetero}}$  were little different from those of  $P\equiv P_{\text{homo}}$ ,<sup>6</sup> indicating that the intrinsic electronic properties of their core units are substantially identical to one other. Hence, the n- and p-type semiconducting natures, observed for the LC states of  $P\equiv P_{\text{hetero}}$  and  $P\equiv P_{\text{homo}}$ , respectively, most likely originate from the different geometries of their  $\pi$ -stacked core units, directed by the side chains (Figure 3). This notion suggests an interesting possibility that, without attaching electron-withdrawing or -donating groups to the electroactive core, both n- and p-type organic semiconductors are available

from single  $\pi$ -conjugated motifs. In relation to this possibility, Brédas and co-workers reported in 2002 a theoretical prediction<sup>15a</sup> that assembled  $\pi$ -conjugated motifs possibly switch their preference for carrier species by changing the  $\pi$ -stacking geometry.<sup>15</sup> However, clear experimental supports have not been provided so far.

In conclusion, we demonstrated that the copper complex of a triply fused porphyrin dimer, when differently decorated at its periphery with appropriate side chains, can afford both n- and p-type liquid crystalline semiconductors ( $P\equiv P_{\text{hetero}}$  and  $P\equiv P_{\text{homo}}$ , respectively), where the side chains employed hardly change the intrinsic  $\pi$ -electronic properties but change the stacking geometry of the core. Although effects of assembly-directing side chains on charge-carrier mobilities have been recognized for several LC semiconductors,<sup>16</sup> nearly perfect switching of carrier species, as demonstrated for  $P\equiv P_{\text{hetero}}$  and  $P\equiv P_{\text{homo}}$ , is unprecedented. This finding is quite encouraging for diversification of organic semiconductors from limited available structural motifs.

## ■ ASSOCIATED CONTENT

**S Supporting Information.** Details of synthesis and characterization of fused metalloporphyrin derivatives, MALDI–TOF mass and NMR spectra, X-ray diffraction patterns, electronic absorption spectra, time-of-flight data, and spectral simulation. This material is available free of charge via the Internet at <http://pubs.acs.org>.

## ■ AUTHOR INFORMATION

### Corresponding Author

aida@macro.t.u-tokyo.ac.jp

## ■ ACKNOWLEDGMENT

The synchrotron radiation experiments were performed at BL02B2 and BL44B2<sup>17</sup> in SPring-8 with the approval of JASRI (Proposal No. 20090021, the Budding Researchers Support Proposal) and RIKEN (Proposal No. 2009A1651, the Priority Nanotechnology Support Program), respectively. T.S. thanks the Japan Society for the Promotion of Science for a Young Scientist Fellowship.

## ■ REFERENCES

- (1) (a) Pron, A.; Gawrys, P.; Zagorska, M.; Djurado, D.; Demadrille, R. *Chem. Soc. Rev.* **2010**, *39*, 2577–2632. (b) Brédas, J.-L.; Beljonne, D.; Coropceanu, V.; Cornil, J. *Chem. Rev.* **2004**, *104*, 4971–5003.
- (2) (a) Katz, H. E.; Bao, Z.; Gilat, S. L. *Acc. Chem. Res.* **2001**, *34*, 359–369. (b) Zaumseil, J.; Sirringhaus, H. *Chem. Rev.* **2007**, *107*, 1296–1323. (c) Wu, W.; Liu, Y.; Zhu, D. *Chem. Soc. Rev.* **2010**, *39*, 1489–1502.
- (3) (a) Tsuda, A.; Furuta, H.; Osuka, A. *Angew. Chem. Int. Ed.* **2000**, *39*, 2549–2552. (b) Tsuda, A.; Osuka, A. *Science* **2001**, *293*, 79–82. (c) Ikeda, T.; Aratani, N.; Osuka, A. *Chem. Asian J.* **2009**, *4*, 1248–1256.
- (4) Sakurai, T.; Shi, K.; Sato, H.; Tashiro, K.; Osuka, A.; Saeki, A.; Seki, S.; Tagawa, S.; Sasaki, S.; Masunaga, H.; Osaka, K.; Takata, M.; Aida, T. *J. Am. Chem. Soc.* **2008**, *130*, 13812–13813.
- (5) (a) Hains, A. W.; Liang, Z.; Woodhouse, M. A.; Gregg, B. A. *Chem. Rev.* **2010**, *110*, 6689–6735. (b) Zimmerman, J. D.; Diev, V. V.; Hanson, K.; Lunt, R. R.; Yu, E. K.; Thompson, M. E.; Forrest, S. R. *Adv. Mater.* **2010**, *22*, 2780–2783.
- (6) See Supporting Information.
- (7) (a) Percec, V.; Johansson, G.; Ungar, G.; Zhou, J. *J. Am. Chem. Soc.* **1996**, *118*, 9855–9866. (b) Percec, V.; Glodde, M.; Peterca, M.;

Rapp, A.; Schnell, I.; Spiess, H. W.; Bera, T. K.; Miura, Y.; Balagurusamy, V. S. K.; Aqad, E.; Heiney, P. H. *Chem. Eur. J.* **2006**, *12*, 6298–6314. (c) Tschierske, C. *Chem. Soc. Rev.* **2007**, *36*, 1930–1970. (d) Lehmann, M. *Chem. Eur. J.* **2009**, *15*, 3638–3651.

(8) Lehmann, M.; Jahr, M.; Gutmann, J. *J. Mater. Chem.* **2008**, *14*, 2995–3003.

(9) (a) Yang, W. -Y.; Ahn, J. -H.; Yoo, Y. -S.; Oh, N. -K.; Lee, M. *Nat. Mater.* **2005**, *4*, 399–402. (b) Lehmann, M.; Jahr, M.; Donnio, B.; Graf, R.; Gemming, S.; Popov, I. *Chem. Eur. J.* **2008**, *14*, 3562–3576.

(10) (a) Maiti, N. C.; Mazumdar, S.; Periasamy, N. *J. Phys. Chem. B* **1998**, *102*, 1528–1538. (b) Helmich, F.; Lee, C. C.; Nieuwenhuizen, M. M. L.; Gielen, J. C.; Christianen, P. C. M.; Larsen, A.; Fytas, G.; Leclère, P. E. L. G.; Schenning, A. P. H. J.; Meijer, E. W. *Angew. Chem. Int. Ed.* **2010**, *49*, 3939–3942.

(11) Hunter, C. A.; Sanders, J. K. M. *J. Am. Chem. Soc.* **1990**, *112*, 5525–5534.

(12) (a) Shearman, G. C.; Yahioglu, G.; Kirstein, J.; Milgrom, L. R.; Seddon, J. M. *J. Mater. Chem.* **2009**, *19*, 598–604. (b) Ohta, K.; Yamaguchi, N.; Yamamoto, I. *J. Mater. Chem.* **1998**, *8*, 2637–2650.

(13) Similar to the case of  $\text{P}\equiv\text{P}_{\text{hetero}}$ , the time-of-flight profile of its TEG version, newly obtained, showed a small p-type signature along with the n-type conducting feature (Figure S11). Although this ambipolar profile was more explicit than that of  $\text{P}\equiv\text{P}_{\text{hetero}}$ , the hole mobility estimated was several times smaller than the electron mobility.

(14) (a) Saeki, A.; Seki, S.; Sunagawa, T.; Ushida, K.; Tagawa, S. *Philos. Mag.* **2006**, *86*, 1261–1276. (b) Saeki, A.; Seki, S.; Takenobu, T.; Iwasa, Y.; Tagawa, S. *Adv. Mater.* **2008**, *20*, 920–923.

(15) (a) Cornil, J.; Lemaury, V.; Calbert, J. P.; Brédas, J.-L. *Adv. Mater.* **2002**, *14*, 726–729. (b) Lemaury, V.; Da Silva Filho, D. A.; Coropceanu, V.; Lehmann, M.; Geerts, Y.; Piris, J.; Debije, M.; Van de Craats, A.; Senthilkumar, K.; Siebbeles, L.; Warman, J.; Brédas, J.-L.; Cornil, J. *J. Am. Chem. Soc.* **2004**, *126*, 3271–3279. (c) Marcon, V.; Breib, D. W.; Pisula, W.; Dahl, J.; Kirkpatrick, J.; Patwardhan, S.; Grozema, F.; Andrienko, D. *J. Am. Chem. Soc.* **2009**, *131*, 11426–11432. (d) Cornil, J.; Brédas, J.-L.; Zaumseil, J.; Sirringhaus, H. *Adv. Mater.* **2007**, *19*, 1791–1799.

(16) (a) Feng, X.; Marcon, V.; Pisula, W.; Hansen, M. R.; Kirkpatrick, J.; Grozema, F.; Andrienko, D.; Kremer, K.; Müllen, K. *Nat. Mater.* **2009**, *8*, 421–426. (b) Li, W.-S.; Yamamoto, Y.; Fukushima, T.; Saeki, A.; Seki, S.; Tagawa, S.; Masunaga, H.; Sasaki, S.; Takata, M.; Aida, T. *J. Am. Chem. Soc.* **2008**, *130*, 8886–8887. (c) Iino, H.; Hanna, J.; Bushby, R. J.; Movaghar, B.; Whitaker, B. J.; Cook, M. *Appl. Phys. Lett.* **2005**, *87*, 132102.

(17) Kato, K.; Hirose, R.; Takemoto, M.; Ha, S.; Kim, J.; Higuchi, M.; Matsuda, R.; Kitagawa, S.; Takata, M. *AIP Conf. Proc.* **2010**, *1234*, 875–878.